

Tunable current circulation in triangular quantum-dot metastructures

Chen-Yen Lai,^{1,2} Massimiliano Di Ventra,³ Michael Scheibner,⁴ and Chih-Chun Chien^{4,*}

¹*Theoretical Division, Los Alamos National Laboratory, Los Alamos, New Mexico 87545, USA*

²*Center for Integrated Nanotechnologies, Los Alamos National Laboratory, Los Alamos, New Mexico 87545, USA*

³*Department of Physics, University of California, San Diego, La Jolla, CA 92093, USA.*

⁴*School of Natural Sciences, University of California, Merced, Merced, CA 95343, USA.*

(Dated: December 3, 2024)

Advances in fabrication and control of quantum dots allow the realization of metastructures that may exhibit novel electrical transport phenomena. Here, we investigate the electrical current passing through one such metastructure, a system composed of quantum dots placed at the vertices of a triangle. We uncover the relation between its steady-state total current and the internal current circulation within the metastructure in the absence of any external magnetic field. By calculating the electronic correlations in quantum transport exactly, we present phase diagrams showing where different types of current circulation can be found as a function of the correlation strength and the coupling between the quantum dots. Finally, we show that the regimes of current circulation can be further enhanced or reduced depending on the local spatial distribution of the interactions, suggesting a single-particle scattering mechanism is at play even in the strongly-correlated regime. We suggest experimental realizations of actual quantum-dot metastructures where our predictions can be directly tested.

Quantum transport is an important area of research with a wide range of phenomena and applications, especially in fields like condensed-matter [1, 2] and cold-atom systems [3–7]. Of particular present interest are those phenomena that emerge in the presence of nontrivial geometry or topology. The prototypical example is the Aharonov-Bohm (AB) effect [8] which arises when a finite vector potential is encircled by a conducting ring and endows the electron wave-function with an additional geometrical phase. However, several other interesting transport phenomena emerge from geometry and topology, such as quantized conduction via edge states of topological insulators that have been an important probe for nontrivial topology in the band structure [9–12], or flat bands of geometrically-induced localized states that interfere with mobile particles and influence their transport [13, 14], to name just a few.

Nanoscale structures, such as quantum dots (QDs), offer additional opportunities to engineer *metastructures* that, if appropriately constructed, may reveal quantum transport phenomena otherwise difficult to probe with other means. Here, we investigate quantum currents through a topologically nontrivial metastructure consisting of QDs placed at the vertices of a triangle with additional elements for tuning the tunneling and interactions. We call it a “triangular quantum-dot metastructure” (TQDM). These metastructures resemble the triangular triple quantum dot, which has been already fabricated and employed in studying other physical properties [15–19] (see below).

To probe the internal electrical dynamics of the TQDM, we connect two of the three QDs to two external reservoirs, as illustrated in Fig. 1(a). Such a system forces the currents to flow through a non simply-connected region, generating current circulation within the TQDM without the need of a vector or scalar potential. The internal circulation is then possible because of the non-trivial topology of the TQDM and the wave nature of quantum particles. In addition, one can detect the emergence of the internal TQDM current circulation by vary-

ing a single link between two of the three QDs, giving rise to a non-monotonic behavior of the total current. By introducing correlations one can tune the circulation further by switching from clockwise (CW) to counterclockwise (CCW) to no-circulation or unidirectional (UD) flow. Computing electronic correlations *exactly* in the Hubbard model, we provide the corresponding phase diagrams of current circulation as a function of correlation strength and inter-dot coupling. We also study the effect of inhomogeneous correlations, that reveal a single-particle scattering mechanism is at play even in the strongly-correlated regime. We report here the results obtained using an open-system, quantum master equation approach. In the Supplemental Information, we report those obtained by a microcanonical (closed-system) formalism [20], showing that the two approaches lead to the same conclusions. The agreement establishes the model-independence of the internal circulation of current in a multi-connected geometry.

Experimental realization - Before embarking on the theoretical aspects of TQDMs, let us first point out how they can be engineered with the appropriate features to observe the phenomena we predict. First, we note that triangular triple quantum dots have been fabricated to study various phenomena such as charge frustration [15] and tunable transport [18]. There are also proposals of using the TQDM to study quantum phase transitions [16, 17], and a thermal transistor where a triangular triple quantum dot is coupled to three reservoirs has also been proposed [19].

TQDMs can be experimentally realized in several ways. The most obvious one relating to electronic transport utilizes electrostatically defined QDs. Here the dots, the barriers between the dots, and the source and drain are controlled by electronic gates which modify the potential landscape of a 2-dimensional electron gas (2DEG). The gates may be created by electron beam lithography [18] or local anodic oxidation [21–24] on top of an epitaxially grown 2DEG semiconductor heterostructure. Figure 1(b) illustrates this approach.

As another experimental realization, we propose a photonic

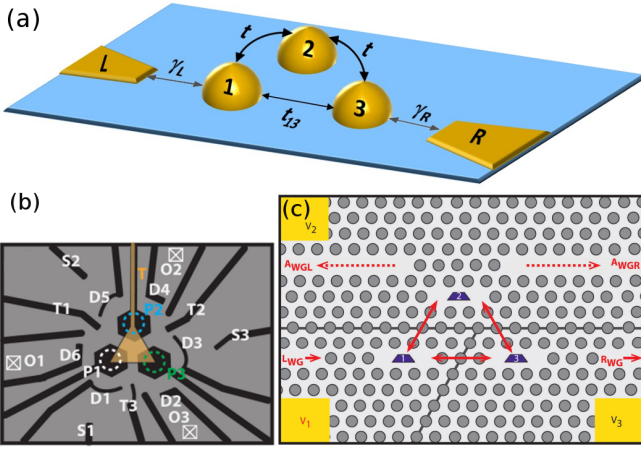


FIG. 1. (a) Schematic rendering of a triangular quantum-dot metas-structure (TQDM) connected to two reservoirs for studying internal current circulation. Here the two reservoirs labeled “L” and “R” are coupled to the TQDM via the coupling $\gamma_{L,R}$, respectively. The tunneling coefficients t and t_{13} are assumed to be tunable. (b) Schematic of a possible experimental structure of a TQDM formed electrostatically in a 2DEG. The design is adapted from [18]. Here, gates T1-T3 control the inter-dot tunneling between dots P1-P3, the (orange) top gate T establishes a depletion region in the center between the dots, gates D1-D6 define the outer boundaries of the three dots, and the additional gates S1-S3 and other contacts can be used for charge sensing. O1-O3 represent Ohmic contacts which serve as leads to/from the QDs. (c) Schematic of possible experimental opto-electronic realization of the TQDM system. The dots are embedded in three L3 cavities in a photonic crystal membrane, formed by a pin-type diode. Photons are injected from the left waveguide (L_{WGL}) and extracted from the right waveguide (R_{WGL}). Additional wave guides (A_{WGL} , A_{WGR}) may be used to measure the directionality of the photon flux. The three dot-cavity systems can be electrically separated from each other by etching through the top p-doped layer of the pin-diode structure. This allows the application of different electric fields via gate voltages V_1 - V_3 , thereby allowing individual tuning of the QD transitions and coupling strengths.

circuit architecture, operated in the photon blockade regime to achieve the required fermionic behavior [25]. An example design is shown in Fig. 1(c). Here, the QDs are embedded in three L3 photonic crystal cavities, which are spatially arranged to create the triangular topology. The source and drain are formed by two photonic crystal waveguides, which guide photons from and to the input and output couplers and couple to the excitons in the quantum dots 1 and 3. Auxiliary waveguides, weakly coupled to dot number 2, may be used to measure the directionality of the “photon” current simulating the electronic current. The fermion spin may be simulated by coupling polarized photons to form polaritons. Coupling between the three cavities depends on the separation, orientation and structural details. (See the SI for more details.)

Theoretical model - To describe the steady-state transport of fermions through the TQDM, we employ an open-system approach and solve a Markovian quantum master-equation by considering a triangular lattice whose site-1 and site-3 are con-

nected to two particle reservoirs via couplings γ_L and γ_R , as illustrated in Fig. 1(a). The left (right) reservoir acts as a particle source (drain) which pumps (removes) particles into (out of) the triangle. Here, we make the assumptions that the coupling between the system and reservoirs is weak in the sense that the frequency scale associated with the coupling between the system and environment is small compared to the dynamical frequency scales of the system or the reservoirs. Moreover, the Markovian approximation requires the coupling to be time-independent and the time evolution of the TQDM to be slow compared to the time necessary for the environment to “forget” quantum correlations [26, 27].

Then, the dynamics can be described by the Lindblad equation ($\hbar = 1$ throughout):

$$\frac{d\rho}{dT} = i[\rho, \mathcal{H}] + \gamma_L \left(c_1^\dagger \rho c_1 - \frac{1}{2} \{c_1 c_1^\dagger, \rho\} \right) + \gamma_R \left(c_3 \rho c_3^\dagger - \frac{1}{2} \{c_3^\dagger c_3, \rho\} \right), \quad (1)$$

where ρ is the density matrix of the TQDM and $\{A, B\}$ denotes the anticommutator of A and B .

We choose as Hamiltonian, \mathcal{H} , of the TQDM that of a single-band triangular lattice with on-site interactions:

$$\mathcal{H} = \sum_{\sigma} \mathcal{H}_{\text{tri},\sigma} + \sum_{p=1}^3 U_p n_{p\uparrow} n_{p\downarrow}, \quad (2)$$

where

$$\mathcal{H}_{\text{tri},\sigma} = -t(c_{1\sigma}^\dagger c_{2\sigma} + c_{2\sigma}^\dagger c_{3\sigma} + h.c.) - t_{13}(c_{1\sigma}^\dagger c_{3\sigma} + c_{3\sigma}^\dagger c_{1\sigma}). \quad (3)$$

Here, $c_{n\sigma}^\dagger$ ($c_{n\sigma}$) is the fermion creation (annihilation) operator on site n and $\sigma = \uparrow, \downarrow$ denotes the spin. The number operator of the spin σ fermions on site p is $n_{p\sigma} = c_{p\sigma}^\dagger c_{p\sigma}$. The coupling between QD 1 and 3 is labeled t_{13} , which can be tuned independently of the other coupling, t , between QDs 1 and 2, and QDs 2 and 3. The correlation strength, U_p , can also be tuned for each QD independently. The time unit is $T_0 \equiv \hbar/t$.

The current operator from site p to site q is given by

$$\hat{j}_{pq} = -i \sum_{\sigma} (t_{pq} c_{p\sigma}^\dagger c_{q\sigma} - h.c.). \quad (4)$$

Here t_{pq} is the hopping coefficient from p to q . In this work we consider the zero-temperature limit. The current on the link from site p to site q of the triangular lattice can be extracted from the off-diagonal elements of the single-particle correlation matrix $\langle C_{pq\sigma} \rangle = \langle c_{p\sigma}^\dagger c_{q\sigma} \rangle$ as $j_{pq} = -2 \sum_{\sigma} \text{Im} \langle t_{pq} C_{pq\sigma} \rangle$. In the following we choose $\gamma_L = \gamma_R = \gamma$ and focus on the steady state where $d\rho/dT = 0$ in the long-time limit ($T \rightarrow \infty$), and a steady-state current can be identified. We now analyze both the total current flowing through the triangle and the internal currents inside the triangle, by varying t_{13} within the triangle, the system-reservoir coupling γ , and the strength of the interaction U_p . Details of the calculations can be found in the SI as well as confirmation of these results using a micro-canonical approach.

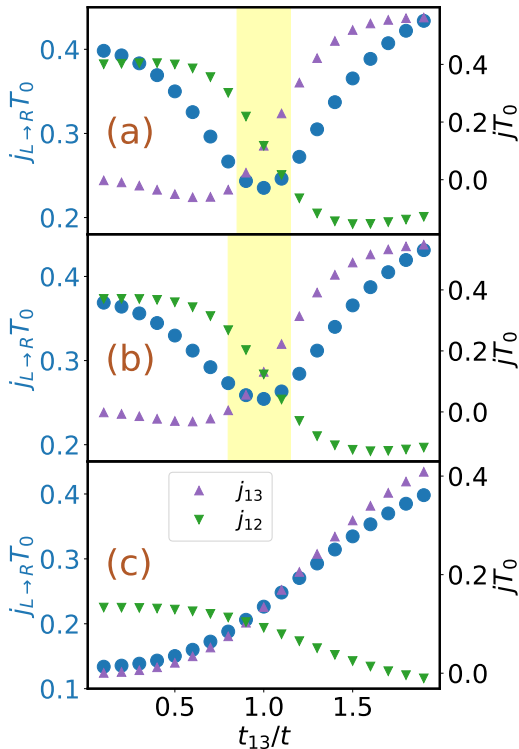


FIG. 2. Steady-state currents versus different hopping coefficient t_{13} of the triangular lattice connected to two reservoirs modeled as an open quantum system with $\gamma T_0 = 1$ and different interaction strengths (a) $U = 0$, the noninteracting case, (b) $U = 1t$, and (c) $U = 5t$. Here $T_0 \equiv \hbar/t$. The solid circles show the total current through the triangle, and the triangle symbols (upside-down triangle symbols) show the internal currents through the 1-3 (1-2) link. The shaded regions in (a) and (b) emphasize the non-monotonic behavior of the total current. In the shaded regions all the internal currents in the triangle are uni-directional (no circulation).

Noninteracting fermions: In absence of interactions, the Lindblad equation can be expressed in terms of the single-particle correlation matrix $\langle C_{pq} \rangle$ in the Heisenberg picture (see the Supplemental Information), and the equation can be solved exactly. Figure 2 (a) shows the total current through the triangular lattice for different values of t_{13} . The total current is not monotonic as t_{13} increases. By examining the internal currents flowing through the upper (1-2-3) and lower (1-3) branches of the triangle (Fig. 1a), we find indeed internal current circulation in the triangle. Here the CW (CCW) circulation has an opposite current flowing along the path 1-3 (path 1-2-3). We found CW (CCW) circulation when t_{13}/t is small (large), and the bending region of the total current corresponds to the regime where all internal currents flow in the same direction. The non-monotonic behavior of the total current as t_{13} is varied can also be corroborated by the Landauer formalism [2, 28]. (See the SI for details.)

Figure 3(a) shows the phase diagram of the internal currents, where unidirectional, clockwise, and counterclockwise

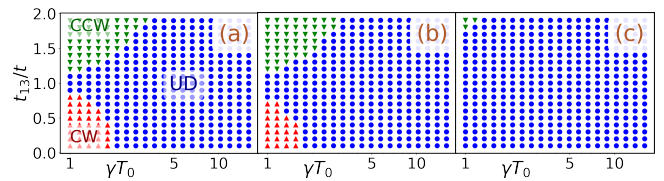


FIG. 3. Phase diagrams of the internal current circulation from the open quantum system approach with different uniform interaction strengths $U = 0, t$, and $5t$ from left to right. The blue circles indicate where all the three internal currents are unidirectional (UD), the red triangle symbols indicate where clockwise (CW) circulating current ($j_{13} < 0$) can be found, and the green upside-down triangle symbols indicate where a counterclockwise (CCW) circulating current ($j_{12} = j_{23} < 0$) can be found.

current flows are clearly distinguishable. Spontaneous circulation of currents in quantum fluids has been found theoretically in ideal Fermi gases passing a constriction [29]. Here, we show that the circulation can be controlled in systems with a multi-connected (triangular) geometry. By further examination, we have found that the critical point where j_{12} is reversed is located at $\gamma_L \gamma_R = 4(t_{13}^2 - t^2)$. (See the Supplemental Information for details.)

Interacting fermions - Having found a clear signature of internal current circulation in the TQDM, we now analyze the role of correlations. Since the Hamiltonian, \mathcal{H} , consists of only three sites, we can compute numerically the dynamics of the density matrix with correlations exactly, using a fourth-order Runge-Kutta algorithm [30].

We first examine the system with uniform interactions $U_p = U, \forall p$. The steady-state currents and their dependence on γ are similar to the noninteracting case. When the interaction is weak, the phase diagram showing different internal flows of currents is qualitatively the same as the diagram of noninteracting systems. However, as the interaction becomes stronger the regimes in the parameter space showing internal current circulation shrink when compared to the noninteracting case, as shown in Fig. 3(b). Therefore, by tuning the onsite interaction one can suppress internal circulation of the current.

As discussed in the noninteracting case, the total current flowing through the triangle forms a dip as t_{13} varies due to a change of the current circulation. The same behavior is found in weakly interacting systems as well. Figure 2(b) shows the total current from the left reservoir to the right one and the shaded region indicates where all internal currents are flowing in the same direction. The total current in both the small and large t_{13} regimes changes monotonically with t_{13} when the internal current is circulating. However, the total current exhibits a dip as the internal circulation changes from CCW to CW across the shaded region. Therefore, non-monotonic behavior of the total current as t_{13} varies indicates a change of the internal circulation of current in both noninteracting and weakly interacting cases. In the strongly interacting regime, the internal circulation of current is severely suppressed as

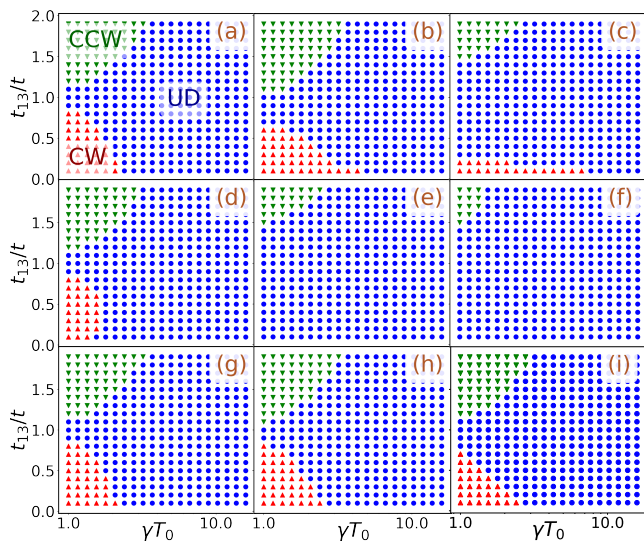


FIG. 4. Phase diagrams of the internal current circulation with non-uniform interactions. The onsite repulsive interaction is only present on (a)-(c) site-1, (d)-(f) site-2, and (g)-(i) site-3, respectively. The local interaction is set to $U = 0.1t$ in the left column, $U = t$ in the central column, and $U = 5t$ in the right column. The labeling of the regimes follows the convention shown in panel (a).

shown in Fig. 3(c), and the total current varies monotonically with t_{13} as shown in Fig. 2(c).

To investigate further how correlations suppress the internal circulation of current, we assume the onsite repulsive interaction is present only on one site, while the other two sites remain noninteracting. The phase diagrams showing where internal circulations can be found in this case are summarized in Fig. 4. The presence of interactions on site 1 affects the clockwise circulation when the interaction is strong as shown in the $U = 5t$ case in Fig. 4(c), but the CCW circulation is less affected. In contrast, if the interaction is only on site 2, the suppression shown in Fig. 4(e) and (f) is similar to the uniform interaction case shown in Fig. 3(c). Finally, the interaction on site-3 has almost no observable influence on the circulation as shown in Fig. 4(g)-(i). Therefore, the dominant interaction effect comes from site-2, and it is possible to reduce the three-state circulation (CCW, CW, and UD) to two-state circulation (CCW and UD) as shown in Fig. 4(e).

The result suggests that scattering of quantum particles is the main mechanism for tuning the internal circulation of current. That this is the case, can be understood as follows. In the presence of interactions on site 2, particles are scattered from that vertex, so the current flowing through the upper (1-2-3) path is reduced. This makes the CW circulation unfavorable because it requires a large current through the upper path and a counter-flowing current on the lower (1-3) path. On the other hand, adding scattering mechanisms like onsite interaction to site 1 or 3 leaves the phase diagrams intact (or completely suppresses the internal circulations). Similar results occur if one includes onsite attractive potentials (see the

SI), thus confirming the single-particle scattering mechanism we have just described. Inhomogeneous interactions or onsite potentials may be achievable in quantum dots coupled to cavities by tuning the photon-exciton coupling. In this respect, the photonic-circuit structure shown in Fig. 1(c) has an advantage over the electrostatic quantum dots when it comes to configurations with tunable inhomogeneity.

Conclusions - We have considered a triangular quantum-dot metastructure connected to two reservoirs and studied the relation between its steady-state total current and its internal current circulation. Internal circulation of current in the triangle are discovered in both closed- and open- system approaches, and the direction can be tuned by a variety of parameters including the hopping coefficient, local interactions or potential, and system-reservoir coupling. Therefore, the internal current circulation model-independent. Moreover, the overall current exhibits non-monotonic behavior when the the circulation reverses. The phase diagrams showing how the circulation can be tuned will assist designs of quantum devices utilizing the internal circulation of current.

Importantly, our findings are not limited to quantum dots because the generic formalism establishes the robustness of the internal current circulation in quantum transport. It is also possible to use the recently developed lattice fermion simulators based on superconducting elements [31] or ultracold atoms in engineered reservoirs and constrictions [32] to explore similar transport phenomena in other controllable quantum systems.

Acknowledgment: We thank Mekena Metcalf for useful discussions. C.Y.L. acknowledges the support from the U.S. Department of Energy through the Center for Integrated Nanotechnologies, a basic energy science user facility. M.S. acknowledges support from the Defense Threat Reduction Agency (Grant No. HDTRA1-15-1-0011) and the Air Force Office of Scientific Research (Grant No. FA9550-16-1-0278). The simulations were performed by the MERCED Cluster in UC Merced supported by the National Science Foundation (Grant No. ACI-1429783).

* cchien5@ucmerced.edu

- [1] S. Datta, *Quantum Transport: Atom to Transistor* (Cambridge University Press, Cambridge, UK, 2005).
- [2] M. Di Ventra, *Electrical Transport in Nanoscale Systems* (Cambridge University Press, Cambridge, 2008).
- [3] C.-Y. Lai and C.-C. Chien, *Phys. Rev. A* **96**, 033628 (2017).
- [4] L. Amico and M. G. Boshier (2015), 1511.07215.
- [5] M. K. Olsen and A. S. Bradley, *Phys. Rev. A* **91**, 043635 (2015).
- [6] C.-C. Chien, S. Peotta, and M. Di Ventra, *Nat. Phys.* **11**, 998 (2015).
- [7] C.-Y. Lai and C.-C. Chien, *Sci. Rep.* **6**, 37256 (2016).
- [8] Y. Aharonov and D. Bohm, *Phys. Rev.* **115**, 485 (1959).
- [9] M. Z. Hasan and C. Kane, *Rev. Mod. Phys.* **82**, 3045 (2010).
- [10] X.-L. Qi and S.-C. Zhang, *Rev. Mod. Phys.* **83**, 1057 (2011).
- [11] S.-Q. Shen, *Topological Insulators: Dirac Equation in Condensed Matters*, vol. 174 (Springer, 2012).

- [12] J. K. Asbóth, L. Oroszlány, and A. Pályi, *A Short Course on Topological Insulators: Band-structure topology and edge states in one and two dimensions* (Springer, Berlin, Germany, 2016).
- [13] M. Metcalf, G.-W. Chern, M. Di Ventra, and C.-C. Chien, *J. Phys. B: At. Mol. Opt. Phys.* **49**, 075301 (2016).
- [14] C.-Y. Lai and C.-C. Chien, *Phys. Rev. Applied* **5**, 034001 (2016).
- [15] M. Seo, H. K. Choi, S. Y. Lee, N. Kim, Y. Chung, H. S. Sim, V. Umansky, and D. Mahalu, *Phys. Rev. Lett.* **110**, 046803 (2013).
- [16] A. K. Mitchell and D. E. Logan, *Phys. Rev. B* **81**, 075126 (2010).
- [17] S. H. Kim, C. J. Kang, Y. I. Kim, and K. H. Kim, *Physica B* **465**, 55 (2015).
- [18] A. Noiri, K. Kawasaki, T. Otsuka, T. Nakajima, J. Yoneda, S. Amaha, M. R. Delbecq, k. Takeda, G. Allison, A. Ludwig, et al., *Semicond. Sci. Technol.* **32**, 084004 (2017).
- [19] Y. Zhang, Z. Yang, X. Zhang, L. B. G. Lin, and J. Chen, *Coulomb-coupled quantum-dot thermal transistors* (2017), arXiv: 1712.06889.
- [20] M. Di Ventra and T. N. Todorov, *J. Phys.: Condens. Matter* **16**, 8025 (2004).
- [21] M. Ishii and K. Matsumoto, *Jpn. J. Appl. Phys.* **34**, 1329 (1995).
- [22] R. Held, S. Luscher, T. Heinzel, K. Ensslin, and W. Wegscheider, *Appl. Phys. Lett.* **75**, 1134 (1999).
- [23] U. F. Keyser, H. W. Schumacher, U. Zeitler, and R. J. Haug, *Appl. Phys. Lett.* **76**, 457 (2000).
- [24] M. C. Rogge and R. J. Haug, *Phys. Rev. B* **77**, 193306 (2008).
- [25] K. M. Bimbaum, A. Boca, R. Miller, A. D. Booze, T. E. Northup, and H. J. Kimble, *Nature* **436**, 87 (2005).
- [26] H.-P. Breuer and F. Petruccione, *The Theory of Open Quantum Systems* (Oxford University Press, Oxford UK, 2002).
- [27] U. Weiss, *Quantum Dissipative Systems* (World Scientific, Singapore, 2012).
- [28] R. Landauer, *IBM J. Res. Dev.* **1**, 223 (1957).
- [29] M. Beria, Y. Iqbal, M. Di Ventra, and M. Muller, *Phys. Rev. A* **88**, 043611 (2013).
- [30] W. H. Press, S. A. Teukolsky, W. T. Vetterling, and B. P. Flannery, *Numerical Recipes 3rd Edition: The Art of Scientific Computing* (Cambridge University Press, New York, NY, USA, 2007), 3rd ed.
- [31] R. Barends, L. Lamata, J. Kelly, L. García-Álvarez, A. G. Fowler, A. Megrant, E. Jeffrey, T. C. White, D. Sank, J. Y. Mutus, et al., *Nat. Comms.* **6**, 7654 (2015).
- [32] M. Lebrat, P. Grisins, D. Husmann, S. Hausler, L. Coerman, T. Giamarchi, P. Brantut, and E. T., *Assembling a mesoscopic lattice in a quantum wire for ultracold fermions* (2017), arXiv: 1708.01250.